Nuclear mean-square charge radii of $^{63,64,66,68-82}$Ga nuclei: No anomalous behavior at $N = 32$

T. J. Procter,[1] J. Billowes,[1] M. L. Bissell,[2] K. Blaum,[3] F. C. Charlwood,[1] B. Cheal,[1,*] K. T. Flanagan,[1,4] D. H. Forest,[5] S. Fritzsche,[6,7] Ch. Geppert,[6,8] H. Heylen,[2] M. Kowalska,[3,9] K. Kreim,[3] A. Krieger,[8] J. Krämer,[8] K. M. Lynch,[1,9] E. Mané,[1] I. D. Moore,[10,11] R. Neugart,[8] G. Neyens,[2] W. Nörtershäuser,[6,8] J. Papuga,[2] M. M. Rajabali,[2] H. H. Stroke,[12] P. Vingerhoets,[2] D. T. Yordanov,[3] and M. Žáková[8]

[1]*School of Physics and Astronomy, The University of Manchester, Manchester M13 9PL, United Kingdom*
[2]*Instituut voor Kern- en Stralingsfysica, KU Leuven, B-3001 Leuven, Belgium*
[3]*Max Planck Institute for Nuclear Physics, Saupfercheckweg 1, 69117 Heidelberg, Germany*
[4]*CSNSM-IN2P3-CNRS, F-91405 Orsay, France*
[5]*School of Physics and Astronomy, The University of Birmingham, Birmingham B15 2TT, United Kingdom*
[6]*GSI Helmholtzzentrum für Schwerionenforschung GmbH, D-64291 Darmstadt, Germany*
[7]*FIAS Frankfurt Institute for Advanced Studies, D-60438 Frankfurt am Main, Germany*
[8]*Institut für Kernchemie, Johannes Gutenberg–Universität Mainz, D-55128 Mainz, Germany*
[9]*Physics Department, CERN, CH-1211 Geneva 23, Switzerland*
[10]*Department of Physics, University of Jyväskylä, FIN-40014 Jyväskylä, Finland*
[11]*Helsinki Institute of Physics, FIN-00014, University of Helsinki, Finland*
[12]*Department of Physics, New York University, New York, New York 10003, USA*

(Received 23 May 2012; published 19 September 2012)

Collinear laser spectroscopy was performed on the $^{63,64,66,68-82}$Ga isotopes with neutron numbers from $N = 32$ to $N = 51$. These measurements were carried out at the ISOLDE radioactive ion beam facility at CERN. Here we present the nuclear mean-square charge radii extracted from the isotope shifts and, for the lighter isotopes, new spin and moment values. New ground-state nuclear spin and moments were extracted from the hyperfine spectra of ^{63,70}Ga, measured on an atomic transition in the neutral atom. The ground-state spin of ^{63}Ga is determined to be $I = 3/2$. Analysis of the trend in the change in mean-square charge radii of the gallium isotopes demonstrates that there is no evidence of anomalous charge radii behavior in gallium in the region of $N = 32$.

DOI: 10.1103/PhysRevC.86.034329 PACS number(s): 21.10.Ky, 21.10.Gv, 27.50.+e, 31.30.Gs

I. INTRODUCTION

Laser spectroscopy allows the study of nuclear ground-state (gs) properties with high precision and sensitivity [1]. Analysis of the hyperfine structure and isotope shifts of extensive series of radioactive isotopes can provide model-independent measurements of the nuclear spin, magnetic dipole and electric quadrupole moments, and changes in mean-square charge radii. These nuclear observables can be used to understand the effects that take place in the nucleus across an isotopic chain.

Recent measurements of nuclear gs properties of neutron-rich gallium isotopes have been performed at ISOLDE using high-resolution optical spectroscopy. In the odd-even gallium isotopes a lowering of the $\pi f_{5/2}$ orbital relative to the $\pi p_{3/2}$ orbital, as the $\nu g_{9/2}$ orbital is filled, was seen to cause a change in gs spin between ^{79}Ga ($I = 3/2$) and ^{81}Ga ($I = 5/2$) [2]. In the odd-odd gallium isotopes new gs spin values were obtained for ^{74,76,78}Ga [3]. In addition to these results, a new isomeric state was discovered in ^{80}Ga [4] and gs spin and isotope shift measurements were made on ^{82}Ga [5]. We report here an extension of these studies to the neutron-deficient gallium isotopes down to $A = 63$.

The study of the neutron-deficient gallium isotopes was motivated by work done by Lépine-Szily *et al.* [6]. They focused on the anomalous behavior of the matter radii of neutron-deficient isotopes of Ga, Ge, As, Se, and Br. In particular, they noticed a monotonic increase in the rms matter radius of Ga with decreasing neutron number from $N = 36$ to $N = 32$. In gallium, from observation of the first excited state energies of the odd-even isotopes, it was argued that this could not be associated with a change in deformation of the nucleus and could point towards the development of a proton skin. A comparison of behavior can be made by looking at the 2^+ and 4^+ excitation energies of the neighboring Zn and Ge isotopes; see Fig. 1. The effect caused by the $N = 50$ shell closure is observed as well as a smaller one at $N = 38$. However, below that point there is little change in the excitation energies, implying no noticeable change in deformation. Laser spectroscopy is uniquely sensitive to the mean-square charge distribution in the nucleus and can detect changes as small as 0.01 fm^2. If the increase in the matter radii was due to changes in the proton distribution we would expect to observe changes of almost 0.5 fm^2 between isotope neighbors. Therefore, if there is a development of a proton skin within the gallium isotopes with decreasing neutron number, it will be clearly visible by an increase of the mean-square charge radius. This paper will present the charge radii values of the $^{63,64,66,68-82}$Ga nuclei along with previously unmeasured nuclear gs spin and moment values.

*bradley.cheal@manchester.ac.uk

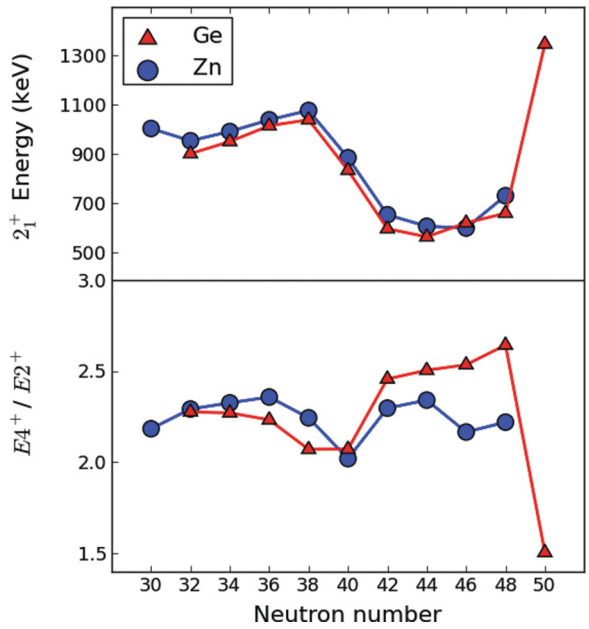

FIG. 1. (Color online) 2_1^+ and $4^+/2^+$ energy levels in Zn (circles) and Ge (triangles) isotopes [7–18]. Noticeable effects are observed at $N = 50$ and $N = 38$; however, no clear effects are seen below $N = 38$.

II. EXPERIMENT

The experiment was performed at the ISOLDE online isotope separator facility at CERN [19]. The radioactive gallium isotopes were produced by impinging 1.4-GeV protons onto the ISOLDE target. For the neutron-deficient isotopes a zirconium oxide target with a reduced titanium concentration, designed to eliminate isobaric titanium oxide contamination [20], was used. Diffusing out of the hot target, the atoms were selectively ionized using the RILIS laser ion source [21]; see Fig. 2. In the RILIS scheme the ground state and the thermally populated 826.24 cm^{-1} metastable state were both excited to the 34781.67 cm^{-1} level and then ionized with 532-nm YAG laser light. The singly charged ions were accelerated to 30 keV, mass separated, and then delivered to the ISOLDE

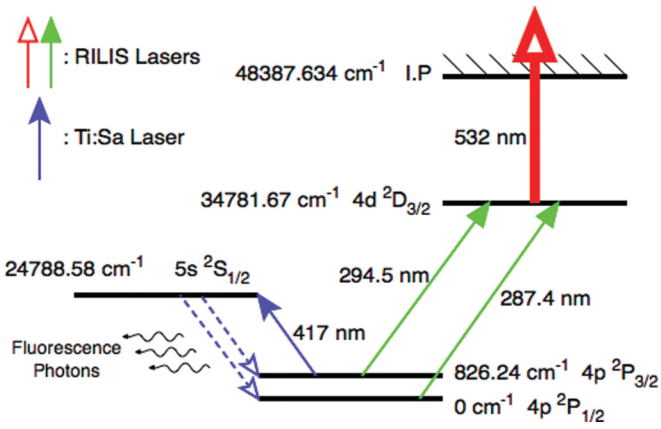

FIG. 2. (Color online) Diagram showing the RILIS ionization scheme [21], along with the excitation transition used to produce the fluorescence photons for detection.

cooler-buncher, ISCOOL [22,23]. The accumulated ions in ISCOOL were released in bunches of 10 μs every 50 ms and then directed towards the COLLAPS experimental beam line [24,25]. The ion beam was first overlapped in a collinear geometry with cw laser light and then neutralized by passage through a charge-exchange channel containing sodium vapor. A frequency stabilized titanium:sapphire laser was operated at 834 nm and frequency doubled to 417 nm in an external cavity in order to drive the $4p\ ^2P_{3/2}$ (826.24 cm^{-1}) $\rightarrow$ $5s\ ^2S_{1/2}$ (24788.58 cm^{-1}) transition; see Fig. 2. The power of the laser was typically 2.5 mW, reduced to minimize optical pumping effects.

An additional acceleration potential was applied to the neutralization cell to allow the hyperfine structure and isotope shift of the atom to be scanned via the Doppler shift. Resonant fluorescence photons were detected using light collection optics and up to four separate photomultiplier tubes, perpendicular to the beam path. A gate on the measurement time corresponding to the passage of the atom bunch along the photomultipliers provided a reduction in the background photon counts, from nonresonantly scattered photons, by a factor of $\sim 10^4$. Measurements were performed with reference scans on stable ^{69}Ga made between each radioactive isotope scan for isotope shift comparisons. Ion beams of isotopes with high yields were attenuated with adjustable slits to ensure the number of ions in each bunch were below 10^7 to avoid space charge effects in the trapping region of the cooler.

III. SPINS AND MOMENTS OF ^{63,70}Ga

The hyperfine structures of ^{63,70}Ga were studied for the first time. The gs spins of the odd-odd isotopes, ^{64,66}Ga, were confirmed as $I = 0$. The odd-even isotopes, ^{65,67}Ga, were not measured to avoid contamination of equipment with long-lived activity. The hyperfine structure was measured for ^{68}Ga; however, the moments are known to be small [26] and the hyperfine splitting thus could not be resolved to extract further information. The gs spin of ^{70}Ga was already known to be $I = 1$ [12] but the magnetic dipole and electric quadrupole moments were unknown. The hyperfine coefficients of ^{70}Ga were extracted from the hyperfine structure using a χ^2 minimization technique, as shown in Fig. 3. The transitions were fitted to Lorentzian profiles and the fitted widths were kept equal for all peaks. The relative intensities of the individual hyperfine components were restricted to angular-momentum coupling estimates [27]. The ratio of the upper and lower hyperfine coefficient A values, $A(^2S_{1/2})/A(^2P_{3/2})$, was restricted to the known value [2] of $+5.592(9)$ for the $4p\ ^2P_{3/2} \rightarrow 5s\ ^2S_{1/2}$ transition, since the hyperfine anomaly was considered to have a negligible effect at this low atomic number [28]. The hyperfine coefficients of ^{70}Ga, along with the calculated nuclear moments, are presented in Table I and Table II, respectively.

In the experiment, several scans were performed on ^{63}Ga to determine the gs spin and moments. The hyperfine structure for all the data sets were analyzed using a χ^2 minimization technique for different possible spin values. A summation of the scans on ^{63}Ga is shown in Fig. 4. The analysis was

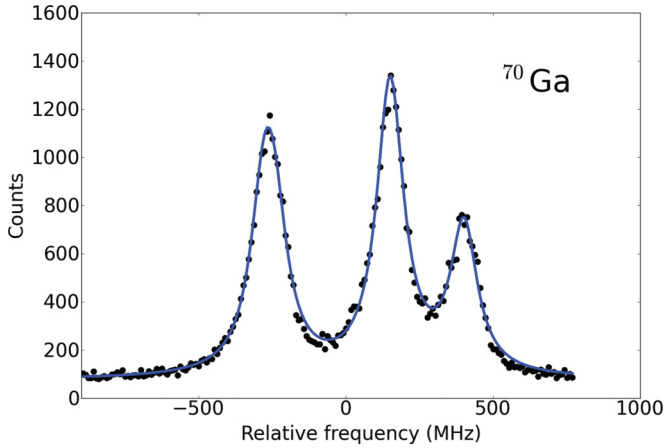

FIG. 3. (Color online) Optical spectrum for ^{70}Ga, $I = 1$, measured on the 417.3 nm, $4p\ ^2P_{3/2}$ (826.24 cm^{-1}) $\rightarrow$ $5s\ ^2S_{1/2}$ (24788.58 cm^{-1}) transition. The data shown is a summation of all scans performed (dots). Included is the fitted spectrum using the extracted hyperfine coefficients of ^{70}Ga and free intensities (solid line).

performed in the same way as for ^{70}Ga, with constrained relative intensities. A preference is shown to $I = 3/2$ ($\chi^2 = 320$); however, the difference from the second best fit of $I = 5/2$ ($\chi^2 = 336$) was not sufficient to reliably assign the spin. To confidently determine the gs spin, a further fitting routine was performed but with the hyperfine coefficients left as free parameters. The ratio of the upper and lower hyperfine coefficient A values, $A(^2S_{1/2})/A(^2P_{3/2})$, were extracted and compared with the known reference value [2] of +5.592(9). The results from this analysis are presented in Table III.

The value produced with the gs spin set at $I = 3/2$ is consistent with the known ratio value of +5.592, whereas for $I = 5/2$ the result differs by 4 standard deviations. Lower laser powers were used to ensure against optical pumping effects, and no bias towards a spin 5/2 assignment was apparent. A gs spin of $I = 1/2$ was ruled out because more than three peaks are present in the hyperfine structure and spins greater than $I = 5/2$ were ruled out as they provided an increasingly poorer match to the known ratio. From this result we can confirm the gs spin of ^{63}Ga as $I = 3/2$. The hyperfine coefficients and moment values were then extracted from the hyperfine structure and are presented in Table I and Table II, respectively.

TABLE I. The measured hyperfine A and B coefficients of ^{63}Ga and ^{70}Ga. The coefficients were extracted from the hyperfine structure using fixed angular-momentum coupling estimates and the ratio of $A(^2S_{1/2})/A(^2P_{3/2}) = +5.592(9)$, obtained from the stable isotopes [2]. For ^{63}Ga it is concluded that the correct gs spin is 3/2 (see Sec. III for details).

A	I	$A(^2S_{1/2})$ (MHz)	$A(^2P_{3/2})$ (MHz)	$B(^2P_{3/2})$ (MHz)
70	1	+454.0(11)	+81.2(2)[a]	+38.3(11)
63	3/2	+778.9(22)	+139.3(4)[a]	+77.5(28)
63	[5/2]	[+525.5(15)]	[+94.0(3)][a]	[+154.5(40)]

[a]Not an independent measurement.

TABLE II. The measured magnetic dipole and electric quadrupole moments of ^{63}Ga and ^{70}Ga. The moments were extracted using the known hyperfine coefficients [2] and magnetic [26] and quadrupole [29] moments of ^{71}Ga for calibration. For ^{63}Ga it is concluded that the correct gs spin is 3/2 (see Sec. III for details).

A	I	μ (μ_N)	Q_s (b)
70	1	+0.571(2)	+0.105(7)
63	3/2	+1.469(5)	+0.212(14)
63	[5/2]	[+1.652(6)]	[+0.424(25)]

IV. SHELL-MODEL CALCULATIONS

The extracted moments of ^{63}Ga were compared with those predicted by shell-model calculations. Two interactions were used for the shell-model calculations: jj44b [2] and JUN45 [30]. The models were developed for the $(p_{3/2}f_{5/2}p_{1/2}g_{9/2})$ model space, assuming a ^{56}Ni core. The magnetic and quadrupole moments obtained are listed in Table IV.

The moment values from the shell models agree well with the experimental results for $I = 3/2$, supporting the wave-function composition, but no correspondence is shown when assuming a spin of $I = 5/2$. This further supports that the gs spin of ^{63}Ga is $I = 3/2$. To further test the models, the ordering of the predicted low-lying energy levels was investigated and are listed in Table V. Each interaction predicts three low-lying energy levels within a few hundred keV of each other and the 5/2 level as the highest and well separated from the gs. The jj44b interaction correctly predicts $I = 3/2$ as the spin of the ground state, with $I = 1/2$ and $I = 5/2$ as the first and second excited states. The JUN45 interaction gives $I = 1/2$ for the ground state. However, this is very close to the $I = 3/2$ state, which is predicted to be within 88 keV of the ground state.

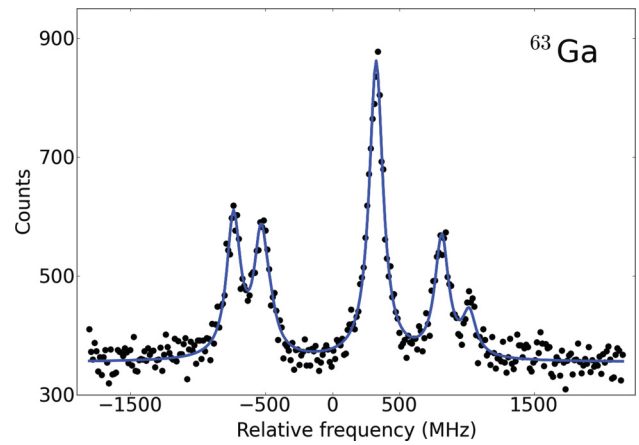

FIG. 4. (Color online) Optical spectrum for ^{63}Ga, $I = 3/2$, measured on the 417.3-nm, $4p\ ^2P_{3/2}$ (826.24 cm^{-1}) $\rightarrow$ $5s\ ^2S_{1/2}$ (24788.58 cm^{-1}) transition. The data shown is a summation of all scans performed (dots). Included is the fitted spectrum using the extracted hyperfine coefficients of ^{63}Ga and free intensities (solid line).

TABLE III. The ratio of the upper and lower hyperfine coefficient A values, $A(^2S_{1/2})/A(^2P_{3/2})$, for fits assuming gs spins of $I = 3/2$ and $I = 5/2$. The difference of the fitted value from the known reference value [2] of +5.592(9) is included.

A	I	$A(^2S_{1/2})/A(^2P_{3/2})$	$A(^2S_{1/2})/A(^2P_{3/2})$
63	3/2	+5.617(30)	+0.025(32)
63	5/2	+5.728(31)	+0.136(33)

V. ISOTOPE SHIFTS

The isotope shift is the difference in the centroid frequency of the hyperfine structure, $\delta\nu_{\rm IS}^{A,A'} = \nu^{A'} - \nu^{A}$, for a pair of isotopes with mass numbers A and A'. Isotope shift values measured in this work on the neutron-deficient Ga isotopes and those measured during previous experiments on the neutron rich isotopes [2–5] are all presented in Table VI. Prior to this work only $\delta\nu_{\rm IS}^{71,69} = +39.6(3.5)$ MHz had been measured [32] and is in excellent agreement with our value in Table VI. In order to extract mean-square charge radii values from isotope shifts two atomic factors need to be evaluated for the transition under study: the atomic mass-shift factor, $K_{\rm MS}$, and field-shift factor, $F_{\rm el}$. These relate the isotope shift to the change in mean-square charge radius, $\delta\langle r_{\rm ch}^2\rangle^{A,A'} = \langle r_{\rm ch}^2\rangle^{A'} - \langle r_{\rm ch}^2\rangle^{A}$, by Ref. [1],

$$\delta\nu_{\rm IS}^{A,A'} = K_{\rm MS}\frac{m_{A'} - m_A}{m_{A'}m_A} + F_{\rm el}\delta\langle r_{\rm ch}^2\rangle^{A,A'}. \qquad (1)$$

The masses, $m_{A'}$ and m_A, used here as well as in the calculation of the Doppler shifts involved in isotope shift measurements, were obtained from the Atomic Mass Evaluation 2003 [33].

Charge radii information based on muonic atom data only exists for the two stable gallium isotopes, ^{69}Ga and ^{71}Ga. These values produce a single value of $\delta\langle r_{\rm ch}^2\rangle^{71,69} = -0.116(20)$ fm^2 [34], which alone is insufficient to calibrate both atomic factors simultaneously. For this reason, multiconfigurational Dirac-Fock (MCDF) calculations were performed [35] and gave rise to the estimates $F_{\rm el} = +400$ MHz fm^{-2} and $K_{\rm MS} = -431$ GHz u for the field-shift factor and mass-shift factor, respectively. From these estimates, changes in the mean-square charge radii were extracted. The obtained change of -0.34 fm^2 in the mean-square charge radius of ^{69}Ga from ^{71}Ga, however, disagrees with the result from Ref. [34] and clearly overestimates the atomic factors and deserves further theoretical investigation in the future.

While the computation of the field-shift factor appears to be quite stable for a systematically enlarged size of the MCDF wave functions, the mass-shift factor depends critically on correlations among the electrons, and no final convergence could be shown for this parameter. This mass-shift parameter comprises two terms of different sign due to the normal (+396 GHz u) and specific mass-shift (−825 GHz u) and therefore suffers from an incomplete cancellation of different correlation contributions. From the stability of the computations, an uncertainty of at least 15% was assigned to the total mass-shift factor and was therefore adjusted to allow for a better fit of the measured data with the nonoptical results. The new mass-shift factor produced was $K_{\rm MS} = -211.4(210)$ GHz u and the mean-square charge radii results produced from this value are shown in Table VI and Fig. 5.

TABLE IV. Experimental and shell-model comparisons of the magnetic dipole, μ, and electric quadrupole, Q_s, moments of ^{63}Ga, with $I = 3/2$ and $I = 5/2$. The shell-model values were predicted using the jj44b [2] and JUN45 [30] interactions. The shell-model results are in agreement with $I = 3/2$ as the gs spin of ^{63}Ga.

Moment (I)	Expt.	jj44b	JUN45
$\mu(3/2)$ (μ_N)	+1.469(5)	+1.605	+1.205
$Q_s(3/2)$ (b)	+0.212(14)	+0.215	+0.259
$\mu(5/2)$ (μ_N)	+1.652(6)	+0.909	+0.813
$Q_s(5/2)$ (b)	+0.424(25)	−0.425	−0.423

TABLE V. Spins and energies of the first three predicted energy levels of ^{63}Ga, using the jj44b [2] and JUN45 [30] interactions.

Interaction	Ground state	First excited state (keV)	Second excited state (keV)
jj44b	$3/2^-$	$1/2^-$(118)	$5/2^-$(165)
jun45	$1/2^-$	$3/2^-$(88)	$5/2^-$(237)

TABLE VI. Isotope shift values and changes in mean-square charge radii from ^{71}Ga, measured on the 417.3-nm, $4p\ ^2P_{3/2}$ (826.24 cm^{-1}) → $5s\ ^2S_{1/2}$ (24788.58 cm^{-1}) line. The charge radii were extracted using $F_{\rm el} = +400(60)$ MHz fm^{-2}, estimated from medium-scale MCDF computations, and $K_{\rm MS} = -211.4(210)$ GHz u, "tuned" to match muonic data. Statistical errors are shown in parentheses and systematic errors are in square brackets. See Sec. V for discussion on errors.

A	$\delta\nu_{\rm IS}^{71,A}$(MHz)	$\delta\langle r_{\rm ch}^2\rangle^{71,A}$ (fm^2)
63	+121(6)[18]	−0.643(15)[135]
64	+94(7)[15]	−0.579(18)[119]
66	+94(5)[11]	−0.329(13)[75]
68	+46(7)[6]	−0.214(18)[46]
69	+40(4)[4]	−0.116(10)[28][a]
70	+4(4)[2]	−0.096(10)[18]
71	0	0
72	+23(3)[2]	+0.161(8)[26]
73	+15.5(15)[40]	+0.243(4)[42]
74	−32(2)[6]	+0.223(5)[45]
75	−45.3(16)[70]	+0.285(4)[58]
76	−86(2)[9]	+0.276(5)[64]
77	−109.4(15)[110]	+0.308(4)[74]
78	−160(2)[13]	+0.270(5)[78]
79	−186.2(19)[140]	+0.290(5)[87]
80g[b]	−239(4)[16]	+0.242(10)[91]
80m[b]	−232.0(25)[160]	+0.260(7)[92]
81	−271.8(15)[170]	+0.242(4)[99]
82[c]	−222(9)[19]	+0.447(23)[120]

[a]Equal to value derived from muonic data [31].
[b]Ground state and isomeric state tentatively assigned [4].
[c]Error on IS covers all spin options [5].

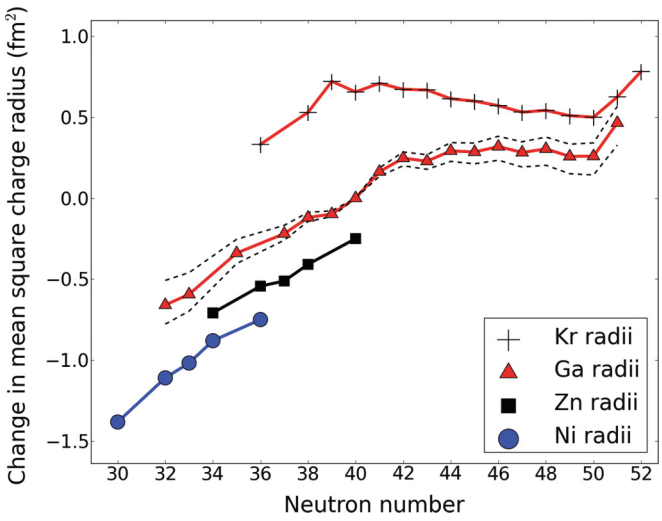

FIG. 5. (Color online) Changes in mean-square charge radii of the gallium isotopes from ^{71}Ga ($N = 40$), plotted alongside relative changes in the neighboring nickel, zinc [31], and krypton [36] isotopes. The neighboring radii have been vertically offset to avoid overlapping of data points and provide the best visible presentation for comparison. The systematic error limits on the gallium radii are represented by the dotted lines.

The error in the K_{MS} value was determined from the uncertainties in the published $\delta\nu_{\mathrm{IS}}^{71,69}$ and $\delta\langle r_{\mathrm{ch}}^2\rangle^{71,69}$ used to calculate the new "tuned" value. For the isotope shifts the systematic errors originate from uncertainties in the acceleration voltage calibration (deviations within 12 V retain consistency with the known $\delta\nu_{\mathrm{IS}}^{71,69}$ value), and for the $\delta\langle r_{\mathrm{ch}}^2\rangle^{71,A}$ values they arise from the uncertainties in the atomic factors. While the acceleration voltage systematic error is included in $\delta\nu_{\mathrm{IS}}^{71,A}$, the effect is incorporated into the "tuned" (effective) K_{MS} factor and cancels in the evaluation of $\delta\langle r_{\mathrm{ch}}^2\rangle^{71,A}$ [37]. To better understand the adjustment of the mass-shift factor, Fig. 5 shows the changes in the charge radii alongside the neighboring Kr, Zn, and Ni isotope chains. The "tuned" K_{MS} factor produces a suitable representation of the slope of the change in charge radii for gallium when compared with the systematic behavior of the other isotopes.

In the Ga isotopes the slope in the change of the mean-square charge radii changes from nearly flat between $N = 42$ and $N = 50$ to strongly downsloping from $N = 42$ down to $N = 32$. No sign of a deviation from this downsloping trend is observed for ^{63}Ga at $N = 32$. If there were any development of a proton skin by ^{63}Ga (as proposed in Ref. [6]), the charge radius would be significantly larger than that of the neighboring isotope. Irrespective of which atomic estimates are used, there is no sign of any sudden deviation in the charge radius by ^{63}Ga and certainly no increase consistent with an increase in matter radius. From these results we therefore can deduce that there is no indication of any anomalous behavior in the neutron-deficient gallium isotopes by ^{63}Ga.

On the neutron-rich side of the chain there is a noticeable effect that occurs at the $N = 50$ shell closure at ^{81}Ga. Here there is a sudden increase in the charge radius from ^{81}Ga to ^{82}Ga, which is also seen in the krypton chain in Fig. 5. This "kink" in the trend is typical of major shell closures. Across both neutron-deficient and -rich sides of the isotope chain there is a small normal odd-N/even-N staggering effect. However, the staggering effect of the radii appears inverted at $N = 40$. The mean-square charge radius of ^{71}Ga (at $N = 40$) appears *smaller* than the average of the neighboring (odd-N) ^{70}Ga and ^{72}Ga isotopes, contrary to the usual trend. This may be indicative of a weak subshell effect at $N = 40$, which (like at $N = 50$) reverses the usual odd-even staggering. A similar effect at this neutron number has also been observed within the copper isotopes [38] and anomalous behavior was seen at $N = 40$ in high-precision mass measurements of Ni, Cu, and Ga [39].

VI. CONCLUSION

From the collation of our and recent experiments on gallium, the majority of the isotopes have now had their ground-state properties measured and the behavior of the charge radii across the chain from $A = 63$ to $A = 82$ has been investigated. New nuclear moment measurements have been made for ^{63,70}Ga and the gs spin of ^{63}Ga has been measured as $I = 3/2$. The charge radii of the neutron-deficient gallium isotopes were investigated and no anomalous behavior was observed at $N = 32$. A shell effect was seen in the charge radii of the neutron-rich gallium isotopes at $N = 50$ as well as a deviation from the normal odd-even staggering at $N = 40$.

ACKNOWLEDGMENTS

This work has been supported by the Science and Technology Facilities Council (UK), the German Ministry for Education and Research (BMBF) under Contract No. 06MZ9178I, Helmholtz Association of German Research Centres (VH-NG-037 and VH-NG-148), the Max-Planck Society, EU Sixth Framework through EURONS (506065), EU Seventh Framework through ENSAR (262010), and the BriX Research Program No. P6/23 and FWO-Vlaanderen (Belgium). E.M. was supported by Conselho Nacional de Desenvolvimento Científico e Tecnológico (CNPq), A.K. by the Carl Zeiss Stiftung (AZ:21-0563-2.8/197/1), and M.K. by the EU (MEIF-CT-2006-042114). We also thank M. Honma and A. Brown for performing shell-model calculations and the ISOLDE technical group for their support and assistance. H.H.S. acknowledges financial aid from the Ed. Scheiderman Fund at NYU.

[1] B. Cheal and K. T. Flanagan, J. Phys. G **37**, 113101 (2010).
[2] B. Cheal, Phys. Rev. Lett. **104**, 252502 (2010).
[3] E. Mané *et al.*, Phys. Rev. C **84**, 024303 (2011).
[4] B. Cheal *et al.*, Phys. Rev. C **82**, 051302 (2010).
[5] B. Cheal *et al.*, J. Phys.: Conf. Ser. **381**, 012071 (2012).
[6] A. Lépine-Szily *et al.*, Eur. Phys. J. A **25**, 227 (2005).
[7] J. K. Tuli, Nucl. Data Sheets **100**, 347 (2003).
[8] H. Junde and B. Singh, Nucl. Data Sheets **91**, 317 (2000).
[9] B. Singh, Nucl. Data Sheets **108**, 197 (2007).
[10] E. Browne and J. K. Tuli, Nucl. Data Sheets **111**, 1093 (2010).

[11] T. W. Burrows, Nucl. Data Sheets **97**, 1 (2002).
[12] J. K. Tuli, Nucl. Data Sheets **103**, 389 (2004).
[13] D. Abriola and A. A. Sonzogni, Nucl. Data Sheets **111**, 1 (2010).
[14] B. Singh and A. R. Farhan, Nucl. Data Sheets **107**, 1923 (2006).
[15] B. Singh, Nucl. Data Sheets **74**, 63 (1995).
[16] A. R. Farhan and B. Singh, Nucl. Data Sheets **110**, 1917 (2009).
[17] B. Singh, Nucl. Data Sheets **105**, 223 (2005).
[18] J. K. Tuli, Nucl. Data Sheets **98**, 209 (2003).
[19] E. Kugler, Hyperfine Interact. **129**, 23 (2000).
[20] E. Prime *et al.*, Hyperfine Interact. **171**, 127 (2006).
[21] B. Marsh *et al.*, Hyperfine Interact. **196**, 129 (2010).
[22] E. Mané *et al.*, Euro. Phys. J. A **42**, 503 (2009).
[23] H. Franberg *et al.*, Nucl. Instrum. Methods **266**, 4502 (2008).
[24] A. Mueller *et al.*, Nucl. Phys. A **403**, 234 (1983).
[25] R. Neugart, Nucl. Instrum. Methods **186**, 165 (1981).
[26] N. J. Stone, Atomic Data and Nuclear Data Tables **90**, 75 (2005).
[27] O. M. Maragó *et al.*, Appl. Phys. B **77**, 809 (2003).
[28] H. H. Stroke, R. J. Blin-Stoyle, and V. Jaccarino, Phys. Rev. **123**, 1326 (1961).
[29] P. Pyykko, Molecular Physics **106**, 1965 (2008).
[30] M. Honma, T. Otsuka, T. Mizusaki, and M. Hjorth-Jensen, Phys. Rev. C **80**, 064323 (2009).
[31] G. Fricke *et al.*, *Nuclear Charge Radii*, Landolt-Börnstein Numerical Data and Functional Relationships in Science and Technology (Springer, Berlin, 2004).
[32] J. Neijzen and A. Dönszelmann, Physica B + C **98**, 235 (1980).
[33] G. Audi *et al.*, Nucl. Phys. A **729**, 337 (2003).
[34] I. Angeli, At. Data Nucl. Data Tables **87**, 185 (2004).
[35] S. Fritzsche, Comput. Phys. Commun. **183**, 1525 (2012).
[36] M. Keim *et al.*, Nucl. Phys. A **586**, 219 (1995).
[37] K. Marinova *et al.*, Phys. Rev. C **84**, 034313 (2011).
[38] M. L. Bissell *et al.* (to be submitted for publication).
[39] C. Guénaut *et al.*, Phys. Rev. C **75**, 044303 (2007).